Biomass and Bioenergy 200 (2025) 108041

Contents lists available at ScienceDirect

Biomass and Bioenergy

journal homepage: www.elsevier.com/locate/biombioe

Pilot scale fast pyrolysis of lignin in a twin-screw reactor

Ana Cristina Corrêa de Araujo [a], Axel Funke [a,*], Antigoni Margellou [b], Konstantinos Triantafyllidis [b], Nicolaus Dahmen [a]

[a] Institute of Catalysis Research and Technology (IKFT), Karlsruhe Institute of Technology (KIT), Hermann-von-Helmholtz Platz 1, 76344 Eggenstein-Leopoldshafen, Germany

[b] Department of Chemistry, Aristotle University of Thessaloniki (AUTH), 54124, Thessaloniki, Greece

ARTICLE INFO

Keywords:
Lignin
Fast pyrolysis
Bio-oil
Twin-screw reactor
Miscanthus
Residue valorization

ABSTRACT

Fast pyrolysis is a promising method for converting lignin into valuable bio-oils, yet it faces significant processing challenges related to melting and agglomeration. In this study, the use of a twin-screw reactor for lignin fast pyrolysis at pilot scale was investigated. The twin-screw reactor design was changed to promote mechanical breakup and better address the issues encountered with melting and agglomeration. Two types of lignin were tested: Indulin AT, a Kraft lignin, and Miscancell, a *Miscanthus*-derived alkali lignin. The experiments with Indulin AT encountered significant challenges related to melting and agglomeration, which ultimately led to its interruption. Changes in the screw reactor design successfully reduced agglomeration inside the reactor, which led to the feeding system becoming the bottleneck for long term operation in terms of agglomeration. In contrast, pyrolysis of the Miscancell lignin proceeded successfully without any agglomeration issues. The difference in processing behavior between the two lignins can be explained by their distinct chemical nature and properties. Analysis of the bio-oils showed that the Indulin AT oil is rich in phenolics, particularly phenols and guaiacols, while the Miscancell oil displayed a broader variety of components, including phenols, guaiacols and syringols, as well as sugars and furans. These findings highlight the potential of the twin-screw reactor for lignin pyrolysis, particularly with Miscancell lignin or similar types that do not exhibit severe melting behavior. However, further optimization of the feeding system is essential to address the issues encountered with Indulin AT, and enable continuous processing of lignins prone to severe melting behavior, such as Kraft lignin.

1. Introduction

Lignin, along with cellulose and hemicellulose, is one of the three main components of lignocellulosic biomass. It is a complex phenolic and aromatic polymer, and it's particularly noteworthy due to its high carbon content and unique chemical structure, making it a promising renewable source of fuels and aromatic chemicals. Lignin is mainly produced as a waste in the pulp and paper industry, during the Kraft process, generating over 50 million tons per year, most of which is simply combusted to recover energy [1]. Additionally, lignin is expected to be produced as a byproduct in the new biorefineries, which can produce biofuels usually through processes aimed at the valorization of biomass sugars [2,3]. Therefore, lignin valorization is essential for developing sustainable biorefineries and advancing the transition towards a bio-based economy.

Fast Pyrolysis is a promising method for converting lignin-rich or isolated lignin biomass into valuable bio-oil and chemicals. The bio-oil derived from lignin is rich in phenolic compounds, which can serve as precursors for the production of high-value chemicals such as phenols, guaiacols, and syringols and BTX aromatics [4,5]. In addition to liquid products, lignin pyrolysis yields biochar, which is gaining increasing attention for its potential in carbon sequestration and soil applications due to its high aromaticity and stability [6]. However, the process is not without challenges. During pyrolysis, lignin tends to soften and melt before it fully decomposes, which leads to processing difficulties, especially in the reactors and feeding systems [7]. Melted lignin can adhere to equipment walls and other surfaces, which can lead to heavy fouling and operational inefficiencies [8]. Moreover, as lignin melts, small particles can stick together, forming larger agglomerates which can cause blockage and clogging of equipment, leading to operational disruptions for cleaning and maintenance, or even shutdown of the process [8].

* Corresponding author.
E-mail address: axel.funke@kit.edu (A. Funke).

https://doi.org/10.1016/j.biombioe.2025.108041
Received 18 December 2024; Received in revised form 21 May 2025; Accepted 28 May 2025
Available online 5 June 2025

One approach to mitigate melting issues involves the pretreatment of lignin with additives, such as calcium hydroxide or mineral clay [9,10]. Such pretreatments have been shown effective in preventing lignin from melting. However, their mechanism of action is not well understood, and they can lead to undesirable side effects, such as increased ash production. In addition, pretreatments can be expensive.

Another strategy to address such challenges is to enhance pyrolysis units by using equipment specifically designed for lignin conversion. Feeding systems can be optimized to work with lignin. Feeding screws can be cooled to prevent lignin from melting, but they only have been proved effective to a certain extent [8,11]. Slug injectors have been tested as feeders for lignin pyrolysis and proven more efficient in preventing melting and blockage [12,13]; the system works by using a pneumatically activated pinch valve to release small amounts of lignin into a tube, forming a slug, then intermittent pulses of inert gas, controlled by a solenoid valve, propel the slug into the reactor.

Reactor selection and design plays a curtail role in the processing of lignin, besides, they also have a great impact on the efficiency, yield, and scalability of the pyrolysis process. Fluidized beds are the most commonly used reactors for lignin fast pyrolysis experiments, but this choice can present challenges for the process [14]. Agglomerates can disrupt the fluidization of particles within the reactor, leading to poor mixing, uneven temperature distribution and in worst cases blockage of the reactor [8]. To overcome problems with bed agglomeration, Gooty et al. [12] and Pienihakkinen et al. [15] inserted a mechanical stirrer inside the fluidized bed to break up the agglomerates formed. Besides fluidized bed, a small number of studies is reported for other types of reactors [14]. The fixed bed reactor has shown promising results but this is only for experiments performed in small scale [16,17]. The pyrolysis centrifuge reactor was successful in pyrolyzing lignin, with rotational forces inhibiting the formation of agglomerates inside the reactor [18]. However, this reactor type may face difficulties when scaling up since its process is surface area dependent. The entrained flow reactor also proved capable to pyrolyze lignin but shows the disadvantages of having poor heat transfer and also being hard to scale up [19].

Auger reactors, though untested for lignin pyrolysis, could potentially be a viable option. Widely applied across slow, intermediate and fast pyrolysis [20–22], they are capable of handling diverse feedstocks, including challenging materials like what straw and *Miscanthus*, validated at Technology Readiness Levels (TRL) 6–7 [23,24]. The twin-screw auger reactor, in particular, may be a good choice due to their enhanced mechanical mixing, which makes them more suitable for sticky and cohesive materials, such as lignin [20]. The screw-driven transport and mixing inherently features mechanical break up [20], which has been proven necessary for processing lignin for pyrolysis in fluidized bed reactors.

The objective of this study is to evaluate the performance of the twin-screw reactor for fast pyrolysis of lignin in terms of yield, efficiency, and operational stability. To address the challenges related to melting and agglomeration, modifications were made to the design of a pre-existing reactor. Specifically, the positions of the biomass and heat carrier inlets were reversed to prevent the lignin from melting on the screw. For the study, two types of lignin were tested: Indulin AT, a Kraft lignin representing the traditional technical lignin from the pulp and paper industry, and Miscancell, a sulfur-free alkali lignin derived from *Miscanthus*, representative of the lignin streams entering the market through alternative biorefinery routes beyond the Kraft process. To validate the yields of the pilot runs and the chemical composition of the bio-oils produced, comparative micro-pyrolysis experiments were conducted. The bio-oils produced were analyzed to determine their physicochemical properties and chemical composition.

2. Materials and methods

2.1. Materials

Two types of lignin were used for the fast pyrolysis experiments. Indulin AT lignin, a purified Kraft lignin from pinewood, free from hemicellulose, manufactured by Ingevity, North Charleston, S.C. USA and supplied by DKSH Switzerland Ltd. And, Miscancell lignin, a sulfur-free lignin extracted from *Miscanthus* via alkaline pretreatment, produced, manufactured, and supplied by Exegi IP Management B.V.

2.2. Micro-pyrolysis experiments

Micro-pyrolysis experiments (Py/GC-MS) were carried out in a Multi-Shot Micro-Pyrolyzer (EGA/PY-3030D, Frontier Laboratories, Japan) connected to a gas chromatographer-mass spectrometer system (GCMS-QP2010, Shimadzu) for fast screening of lignin pyrolysis. For each experiment, a sample of 1 mg of lignin was loaded in a stainless-steel cup, which was quickly dropped into the hot reactor/furnace and pyrolysis was conducted at 500 °C for 12 s. The interface temperature between the micropyrolyzer and GC was set to 320 °C. Helium (99.999 %) was used as the carrier gas at a flow rate of 156 ml/min. The analysis was performed using a capillary column (Ultra Alloy-5, 30 m × 0.25 mm and 0.25 μm film thickness), injector split ratio of 1:150 and column flow 1 ml/min, according to the following temperature program: initial temperature 40 °C, hold for 4 min and heating (5 °C/min) up to 300 °C, hold for 7 min. Both the injector and the detector temperatures were set at 300 °C. The mass spectra were recorded in the range of $m/z = 45–500$ with a scan speed of 5000 amu/s. Identification of mass spectra peaks was achieved using of the scientific library NIST11s. The derived compounds were classified and categorized into 16 groups: mono-aromatics (AR), aliphatics (ALI), phenols (PH), acids (AC), esters (EST), alcohols (AL), ethers (ETH), aldehydes (ALD), ketones (KET), polycyclic aromatic hydrocarbons (PAH's), sugars (SUG) nitrogen compounds (NIT), sulfur compounds (SUL), oxygenated aromatics (OxyAR), oxygenated phenols (OxyPH) and unidentified compounds (UN).

2.3. Fast pyrolysis pilot unit

For the lignin fast pyrolysis experiments, the "*Python*" Processing Development Unit, operated at the Institute of Catalysis Research and Technology at the Karlsruhe Institute of Technology, was used. A flowsheet of the plant can be seen in Fig. 1. The unit operates at a biomass feed rate of 10 kg/h and features a twin-screw mixing reactor that ensures thorough mixing of solid biomass feedstock with a pre-heated heat carrier. The reactor design accommodates a range of feedstocks with varying bulk densities, including lignin powders, without compromising feeding consistency. The residence time of biomass and heat carrier within the reactor is between 10 and 15 s at a rotational frequency of 2 s^{-1} [25]. The heat carrier (steel beads) is recirculated using a bucket elevator to enable continuous flow and consistent thermal conditions, maintaining a heat carrier-to-biomass mass ratio of 100:1. The temperature of the steel beads leaving the reactor, measured as the 'reactor temperature,' is maintained using an electric heater. An inert gas flow (N_2) of 1 m^3/h is supplied during the experiments to maintain an inert atmosphere. Pyrolysis gases, vapors, and char fines are removed from the top of the pyrolysis reactor, with particles separated at reactor temperature in two serial cyclones. The primary product, fast pyrolysis bio-oil, is recovered using a quenching system typically operated at around 90 °C, followed by an electrostatic precipitator. This organic-rich condensate (ORC) is cooled and recirculated to quench the incoming vapor, avoiding the use of an additional quenching medium. In a second condensation step, aqueous condensate (AC) is recovered in a tubular heat exchanger, operated at around 20 °C. Vapors are condensed by direct contact with recirculated and cooled aqueous condensate in a countercurrent flow. Non-condensable gases are

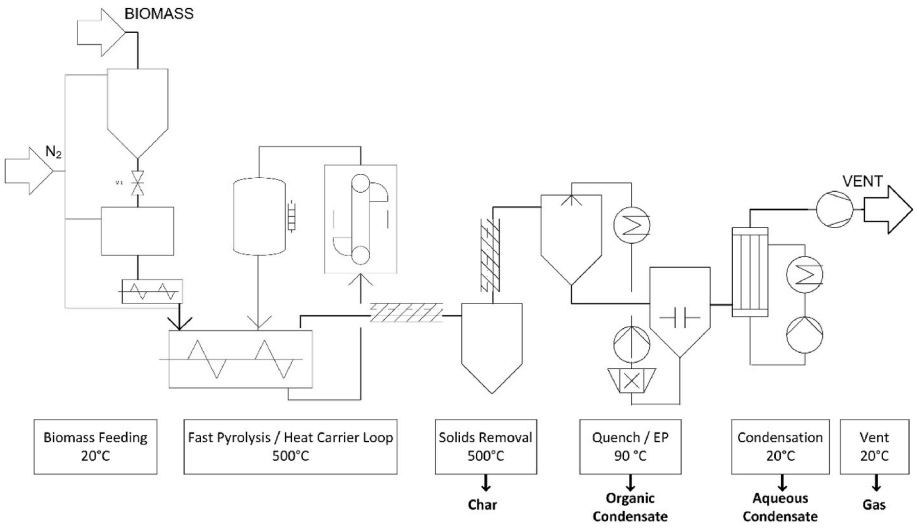

Fig. 1. Flow scheme of Python fast pyrolysis unit [21].

analyzed online by gas chromatography and subsequently vented by a compressor. Gas yields are determined by introducing a tracer gas (neon) with controlled mass flow rate to the reactor. Neon is also quantified by gas chromatography every 15–20 min and the mean of these values are used to determine the gas flow rate over the experiment. The pyrolysis reactor operates under slight underpressure conditions (pressure difference <2 kPa), and the condensation process is similarly under slight underpressure. Ethylene glycol is used as the entrainer material for the first quenching system, while water is used for the second; the mass balance to the condensates refers to the mass of the final product discarding the initial mass of entrainer. A detailed description of the experimental procedure can be found elsewhere [26].

In the original setup of the *Python* unit [21], the feedstock enters the twin-screw reactor at the cold inlet of the screw, while the heat carrier is added later by dropping it onto the feedstock transported by the screws, ensuring fast mixing and minimizing heat losses to the reactor material and the sweeping gas. Although this is not an issue for most biomasses tested in this unit, this arrangement has proven prone to heavy plugging when processing lignin, due to agglomerates forming on the screw shafts. Severe plugging problems were observed in a test run with Indulin AT lignin, leading to complete blockage and shutdown of the unit after just a few minutes of feeding. To mitigate these issues, the feedstock and heat carrier inlets were reversed, as shown in Fig. 2. By dropping the feedstock onto the moving bed of hot steel particles, it is expected that agglomerates will form within the moving bed rather than on the shaft of the screws, where the mechanical agitation could break them up.

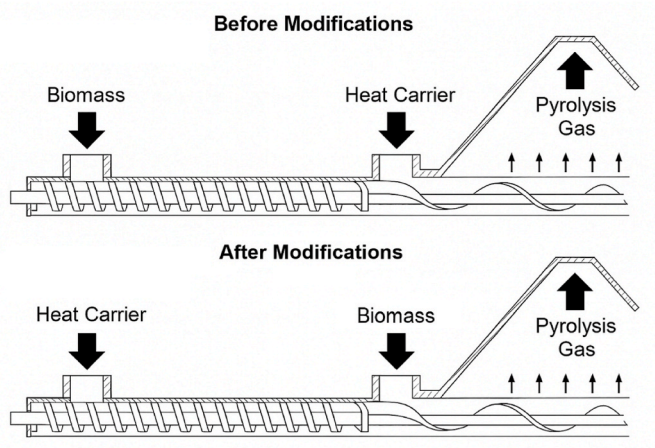

Fig. 2. Scheme of changes to reactor setup to reduce agglomeration at the screw shaft.

Several other hardware modifications were made to facilitate the use of lignin, including adjustment of the gas outlet to avoid fine lignin particles bypassing the agitated bed of heat carrier. Previously, the gas outlet covered the entire length of the reactor from the heat carrier inlet to the solid particle outlet, posing a high risk for shortcut flow of biomass particles if they were inserted instead of the heat carrier particles. The gas outlet was moved to the end of the auger reactor and reduced to a pipe with a small cross-section (around 60 mm). All experiments reported in this manuscript have been conducted with this modified setup.

2.4. Analytical methods

Characterization of the lignin feedstocks and pyrolysis products is crucial for understanding the pyrolysis process and the resulting products. The feedstocks and products were characterized using various techniques. Total solids, moisture, and ash content were determined gravimetrically according to the NREL protocols (NREL/TP-510-42621 and NREL/TP-510-42622) by heating air-equilibrated samples at 105 °C and 575 °C, respectively. Elemental analysis of C/H/N/S content was performed using an Eurovector EA3100 Series CHNS-O analyzer. The oxygen content was calculated by difference. Higher Heating Values (HHV) were computed according to Demirbaş [27] using Eq. (1), where C, H, O, and N, refer to the mass fractions of carbon, hydrogen, oxygen and nitrogen in the material, respectively. Molecular weight of lignins were determined by Gel Permeation Chromatography (GPC), using a Shimadzu Corporation instrument with Shodex KF-801, KF-802.5, and KF-803 columns. THF was used as eluent at 0.5 mL/min, with columns and injection system maintained at 42 °C. Results were given relative to polystyrene standards within the calibration range (162–500.000 Da). Prior to the measurements, lignin were dissolved in THF (1–2 mg/mL) and filtered.

Thermal degradation profiles and residual mass of the lignin feedstocks were determined via thermogravimetric analysis (TGA/DTG). The samples were heated from room temperature to 950 °C at a heating rate of 10 °C/min, under N_2 gas at a flow rate of 50 mL/min. Fourier Transform Infrared Spectroscopy (FTIR) spectra were obtained using a PerkinElmer spectrometer with the KBr pellet method, covering a range of 4000 to 400 cm^{-1}. Inorganic materials were analyzed via Inductively Couple Plasma (ICP) spectroscopy according to the DIN EN ISO 11885 standard. Modified Karl Fischer titration was used to determine water content in the pyrolysis condensates. Gas chromatography-mass

spectrometry/flame ionization detector (GC-MS/FID) analysis of the pyrolysis condensates were performed by the Thünen Institute (Hamburg, Germany), for identification and quantification of components, using internal standards and calibration procedures. A detailed description of the applied method can be found in Windt et al. [28].

Energy balances were calculated based on the mass yields of the pyrolysis products and their respective HHVs. The HHVs of the lignin, ORC and char were estimated according to Eq. (1), using the Demirbaş [27] correlation, and the HHV of the gas was calculated from the gas composition using the standard combustion enthalpy for each species. The aqueous condensate (AC) was excluded from the energy balance due to its high water content and negligible energy contribution.

$$HHV = (33.5[C] + 142.3[H] - 15.4[O] - 14.5[N]) \times 10^{-2} \quad (1)$$

3. Results and discussion

3.1. Lignin characterization

The physicochemical properties of the lignin feedstocks are presented in Table 1, highlighting the differences between Indulin AT and Miscancell lignin. The moisture and ash content in the Miscancell lignin are significantly higher compared to Indulin AT, while elemental analysis indicates that Indulin AT has a higher carbon content than Miscancell, which corresponds to higher lignin content and greater purity, with less ash and fewer cellulose/hemicellulose impurities. Indulin AT also shows the presence of sulfur, expected as it is resulting from the Kraft process, whereas Miscancell is sulfur free, as advertised. On the other hand, Miscancell shows a higher content of nitrogen, which could be attributed to the higher protein content of *Miscanthus* compared to pinewood [29]. Molecular weight values, determined through gel permeation chromatography, suggest that the Indulin AT lignin is composed of larger fractions, while Miscancell is composed of smaller molecules. The similar polydispersity index (PDI) values indicates that both lignin show a broad distribution of molecular weights.

Due to the elevated ash content found in the Miscancell lignin, an inorganic material analysis was conducted. The results of ICP analysis reveal that Miscancell lignin contains more calcium compared to *Miscanthus* samples values from the literature [24,30]. This could be related to the specific *Miscanthus* type used as feedstock for the lignin extraction, or it could be a consequence of the extraction process itself, where the calcium content is increased as it is concentrated in the lignin fraction, while the overall biomass is reduced to about one-third (see Table 2). The high silicon content present in the sample can be attributed to the characteristics of the original biomass. Miscanthus, classified as grass, is known to exhibit high amounts of silicon both through natural uptake and from residual soil or mineral debris during harvesting [30,31]. These sources may contribute to the elevated levels observed and can persist through the lignin isolation process. The content of the other compounds analyzed are consistent with values for *Miscanthus* biomass [24,30].

The thermal decomposition profile of both feedstocks is depicted in the thermogravimetric analysis (TGA) and differential thermogravimetric analysis (DTG) curves shown in Fig. 3 The initial weight loss of 2.4 % for the Indulin AT lignin and 12 % for Miscancell lignin at temperatures up to 120 °C is related to the evaporation of physically adsorbed water molecules (moisture), the numbers are consistent with their moisture content shown in Table 1. The steep weight loss of 39 % for Indulin AT and 46 % for Miscancell in the range of 120 °C–500 °C is attributed to the decomposition of the lignin. The Indulin AT curve resembles a typical lignin decomposition curve, with a wide temperature range and a small decomposition rate, whereas the Miscancell curve shows a high decomposition rate in a rather small temperature interval. The narrow degradation temperature range of Miscancell lignin could be related to its lower molecular weight compared to the Indulin AT [32]. Additional factors, such as its degree of condensation, interlinkages within the structure, and higher inorganic content – which can potentially act as catalysts – may also influence its decomposition behavior [32–34]. Moreover, the small shoulder around the temperature of 250 °C on the Miscancell DTG curve could indicate the presence of hemicellulose impurities in its composition. The residual char produced from the Indulin AT (27 %) and Miscancell (35 %) were consistent with typical lignin values [35]. The higher residual mass of Miscancell lignin can be correlated with the higher content of inorganic materials, in accordance with the higher ash content.

The structural properties of the lignins were determined via FTIR. In the spectra shown in Fig. 4, the characteristic functional groups were identified. Indulin AT lignin exhibits a strong band at 853 cm^{-1} due to deformation vibrations of C-H bonds and at 625 cm^{-1} due to sulfonic groups (C-S) remaining after the Kraft pulping process [36]. Other significant differences between the two lignins are observed in the fingerprint region (800-1700 cm^{-1}). Miscancell lignin shows stronger bands at

Table 2
Inorganic components determined in Miscancell lignin.

Element		Miscancell (ppm)
Aluminum	Al	886
Calcium	Ca	6220
Iron	Fe	851
Potassium	K	6070
Magnesium	Mg	526
Sodium	Na	326
Phosphorus	P	732
Sulfur	S	1430
Silicon	Si	51700
Titanium	Ti	51

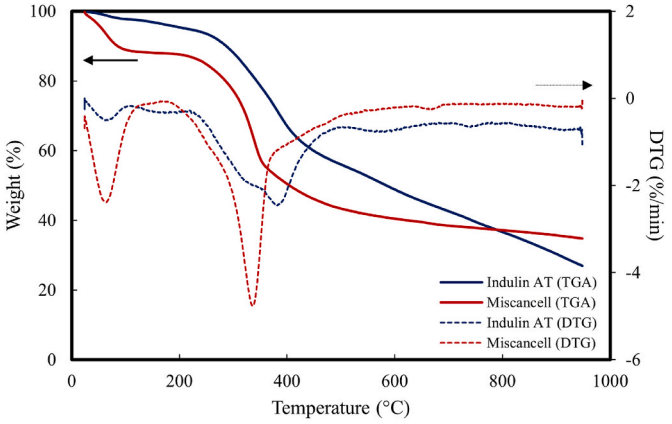

Fig. 3. TGA and DTG curves of Indulin AT and Miscancell lignin.

Table 1
Physicochemical properties of lignin feedstocks.

Lignin Sample	Moisture (wt. %)	Ash[a] (wt. %)	C (wt. %)	H (wt. %)	N (wt. %)	S (wt. %)	O[b] (wt. %)	M_N (g/mol)	M_W (g/mol)	PDI
Indulin AT	4.4	2.4	67.7	6.0	1.0	1.7	21.2	1318	4377	3.3
Miscancell	13.4	14.1	55.8	6.7	2.9	0.0	20.5	844	2587	3.1

[a] Ash content and elemental analysis data are given on dry lignin basis.
[b] Calculated by difference.

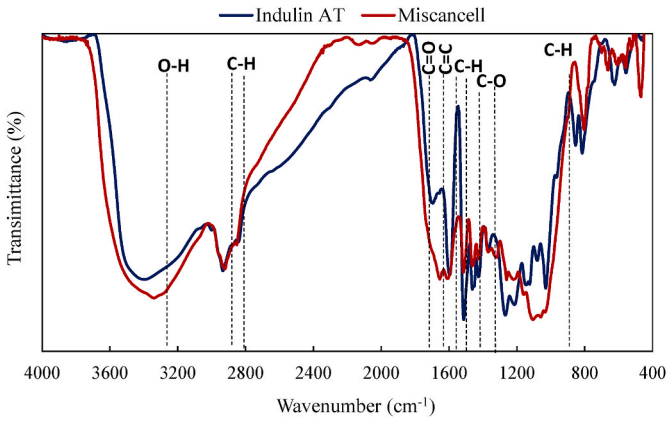

Fig. 4. FTIR of Indulin at and miscancell.

1320 and 1150 cm^{-1}, attributed to syringyl groups, related to its grass nature; In contrast, Indulin AT lignin displays higher intensity bands at 1270, 1030, and 850 cm^{-1}, attributed to guaiacyl units, which are more prominent due to its softwood origin [37].

3.2. Micro-pyrolysis experiments

Micro-scale pyrolysis experiments were performed using the micro pyrolyzer system with on-line GC-MS to investigate the decomposition profiles of lignin and to validate the chemical composition of the bio-oils from the pilot scale runs. The vapor residence time in Py-GC/MS systems is usually much shorter than in larger scale reactors, thus minimizing the secondary reactions which are responsible for char/coke formation, being able to reveal the intrinsic kinetics of lignin fast pyrolysis. On the other hand, the pilot scale reactors refer to relatively longer residence times, allowing (to some extend) secondary reactions thus affecting the products yields (and composition) of liquid oil, gases and char. This combination of scales enables a more complete understanding of lignin pyrolysis, linking intrinsic decomposition behavior with process-scale product distributions. The tests were carried out at 500 °C.

As can be observed in Fig. 5, pyrolysis of Indulin AT identified mainly alkoxylated phenols (OxyPH: 75.8 %), alkoxylated aromatic compounds (OxyAR: 3.9 %), alkylated phenols (PH: 5.6 %) while low amounts of sulfur containing compounds (SUL:1.3 %) were also formed due to the sulfur impurities remained from Kraft pulping. The product distribution obtained within this study is in accordance with other works focused on the pyrolysis of Kraft lignin [38]. Regarding the alkoxylated phenols, all compounds are substituted with one methoxy group, such Guaiacol, 4-vinylguaiacol, Creosol, Isoeugenol, etc. and can be attributed to the softwood nature of pine. The S/G (syringol to guaiacol) ratio of OxyPH is 0/100. For the Miscancell lignin alkoxylated phenols (OxyPH: 56.7 %) and alkoxylated aromatic compounds (OxyAR: 9.4 %) were the most abundant. This lignin also produced more nitrogen containing compounds (NIT: 4.8 %) compared to Indulin AT due to the higher nitrogen content confirmed via elemental analysis. On the other hand, there is the absence of sulfur containing compounds, since the Miscancell lignin is sulfur free. Furthermore, compounds such as sugars (Levoglucosan), furans (Benzofuran, 2,3-dihydro-), acids (acetic acid) are also observed and can be attributed to the degradation of sugar impurities remained from the lignin extraction process [39]. The relative abundance of these compounds accounts for approximately 16 %, suggesting that the carbohydrate content of Miscancell lignin is relatively low. The presence of carbohydrate impurities in Miscancell lignin is also supported by the elemental analysis (Table 1). The weight ratio of C/H is 11.3 for Indulin lignin (similar also to other typical technical lignins) while the ratio for Miscancell lignin is 8.3. The lower C/H ratio indicates the presence of oxygen-rich, non-lignin constituents such as carbohydrates. Regarding the alkoxylated phenols, the five most abundant compounds, shown in Table 3, are substituted with one (guaiacol, 4-vinylguaiacol, Isoeugenol, etc.) and two methoxy groups (syringol), with respect to the grass nature of *Miscanthus*. These results are in line with other studies on Miscanthus-derived lignins, which also report a predominance of guaiacyl and syringyl compounds as major pyrolysis products [40,41]. The S/G ratio of OxyPH is 33/67.

3.3. Fast pyrolysis pilot scale experiments

With the changes to the order of biomass and heat carrier inlets of the reactor completed, the pilot-scale experiments with the new configuration started using the Indulin AT lignin. The modifications successfully reduced blockage inside the reactor and plugging issues were no longer observed in the reactor (see Fig. 6A and B). However, agglomerates started to build up at the inlet of the biomass feeding drop pipe, eventually leading to blockage of biomass supply into the reactor (see Fig. 6C). This is likely due to hot lignin particles being spun off the rotating shaft/heat carrier bed and hitting the relatively cold drop pipe walls. These melted or partially pyrolyzed particles stick to the surface of the pipe, leading to a gradual buildup. The blockage required mechanical breakup, indicating it had solidified and was no longer the original free-flowing material. Since the experiments with the Indulin AT only ran for a short amount of time due to the blockages, steady state and

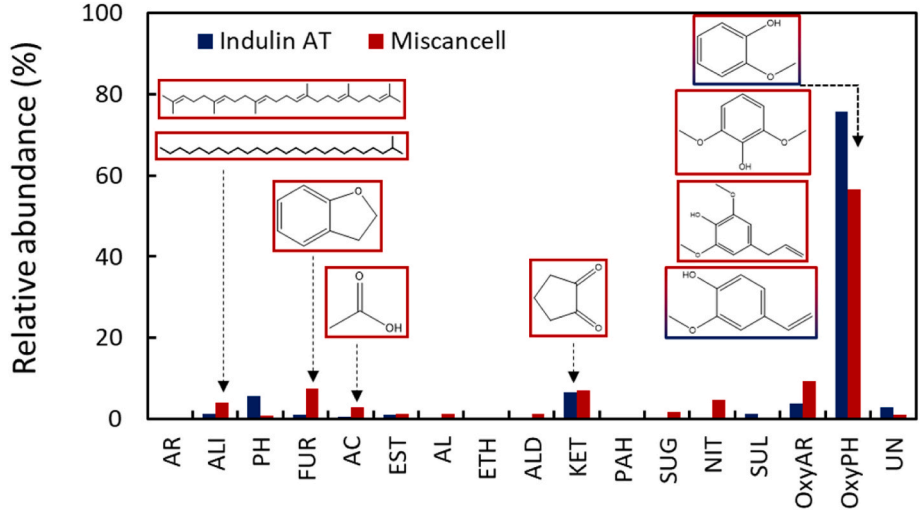

Fig. 5. Relative composition of Indulin AT and Miscancell lignin derived bio-oils in the Py-GC/MS system.

Table 3
Five most abundant compounds identified in lignin's pyrolysis vapors.

Compounds	Structure	Category	Relative abundance (%)
Indulin AT			
Guaiacol		OxyPH	22.9
4-vinylguaiacol	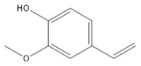	OxyPH	10.9
Creosol	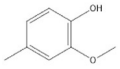	OxyPH	10.5
trans-Isoeugenol	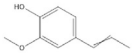	OxyPH	6.7
7-(3,4-Methylenedioxy)-tetrahydrobenzofuranone	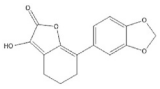	KET	6.6
Miscancell			
4-vinylguaiacol	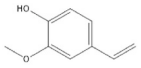	OxyPH	15.6
Syringol	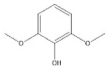	OxyPH	9.3
Guaiacol		OxyPH	9.2
Benzofuran, 2,3-dihydro-	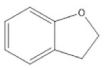	FUR	7.5
3′,5′-Dimethoxyacetophenone	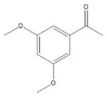	OxyAR	6.6

mass balances were not achieved; still some bio-oil samples were recovered for analysis.

In contrast to Indulin AT, no issues were observed when processing the Miscancell lignin. Visual inspection post-run confirmed the absence of buildup material on the shaft or drop pipe surfaces, as shown in Fig. 7 A and B respectively. The differences in processing the two lignins could be attributed to their distinct chemical nature as well as their physico-chemical properties, such as molecular weight distribution. Higher molecular weights, which is the case for Indulin AT, have been correlated with faster polymerization and higher char yields, which can contribute to agglomeration and processing challenges [42]. On the other hand, Miscancell lignin, with its lower molecular weight and different structural characteristics, processed smoothly with no agglomeration issues, highlighting how specific structural features and properties can significantly influence pyrolysis behavior. Similarly, hydrolysis lignin has been reported to exhibit no severe melting problems [15,32], further supporting the role of the chemical properties in processing outcomes. These observations show how the lignin structure and properties are important for successful processing, as well as the need for further optimization of feeding systems for efficient pyrolysis of different lignin types.

Two batches of the Miscancell lignin were processed in the *Python* unit. The overall experiments were rated as successful, and the mass balances of the runs are summarized in Fig. 8. The ORC and AC yields of the Miscancell lignin experiments (36.5–39.8 wt% and 7.6–10.7 wt%) seem reasonably high; however, they are skewed by a surprisingly high solids content that passed the two serial cyclones as well as high water content. Organic liquid yields are 22.9–29.2 wt% and thus significantly lower that reported by Pienihakkinen et al. [15] (around 40 wt %). It should be noted that the lignin used in the present study contained a high amount of potassium, which is known to catalyze pyrolysis reactions and consequently leads to lower condensate yields [43]. The larger deviations in char and gas yields can be due to an underestimation of gas yield in the Miscancell batch #1 run. However, higher gas and lower solid yields are not typical for such process. One reason for the low char yield could be in char agglomeration in the heat carrier cycle, leading to unaccounted for char not reaching the cyclone systems. This is typically not observed in this unit but might be promoted to liquefied lignin sticking to heat carrier particles and subsequent charring. In larger scale facilities this would not pose a problem since the char is partially burnt and steady state conditions are achieved over a prolonged period [23]. Short term agglomeration of solids in the heat carrier cycle significantly affects the mass balance for the comparably short duration of these pilot runs (3–4 h).

Carbon balance results support the previous observation that conversion to organic liquids was comparably inefficient (see Table 4). Since yields are in a similar range as other feedstocks with high ash content [21], it is likely that the high lignin ash content is causing these low organic liquid yields. Moreover, it is very likely that there was a problem in gas metering during the first Miscancell run.

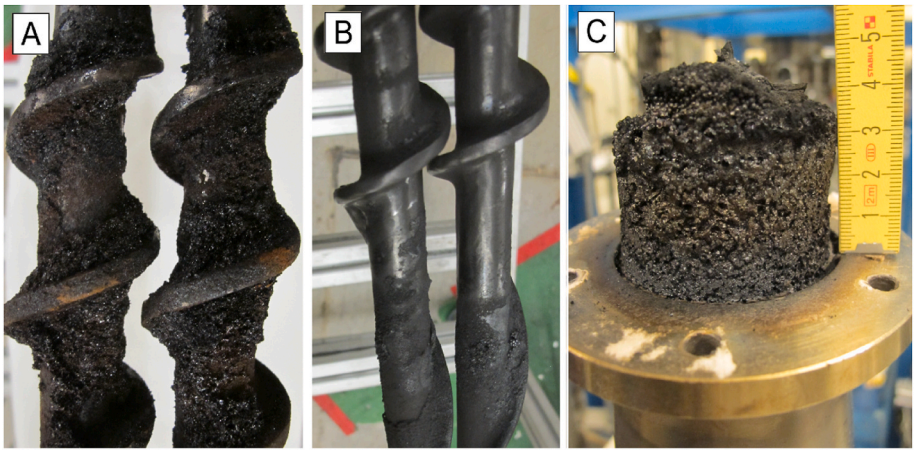

Fig. 6. A) Melted lignin on screw shaft from experiment with Indulin AT before reactor modifications; B) Clean screw shaft and C) Built-up in reactor inlet from the experiment with Indulin AT after reactor modifications.

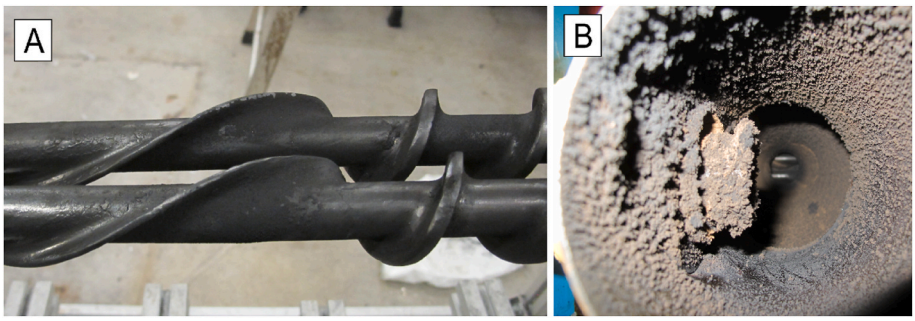

Fig. 7. A) Clean screw shaft and B) Interior of biomass drop pipe (showing no blockage) after the experiment with Miscancell lignin.

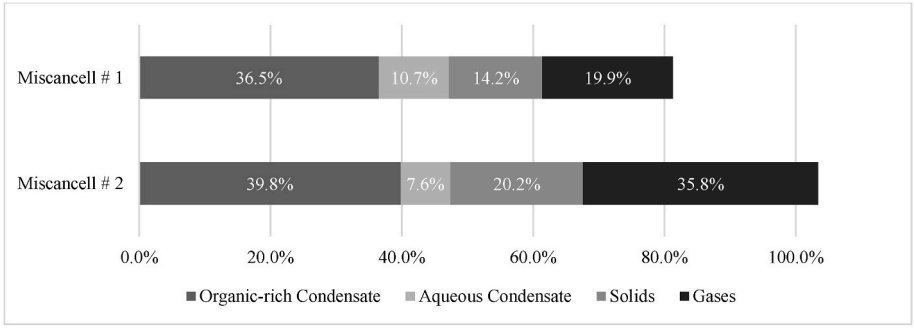

Fig. 8. Mass balances of pilot runs with the Miscancell lignin in wt. %.

Table 4
Carbon balances of lignin fast pyrolysis experiments (wt.% of feedstock carbon).

	Char	ORC[a]	AC	Gases
Miscancell #1	24.3	24.7	4.1	15.6
Miscancell #2	30.8	28.7	4.2	28.7

[a] Excluding solids.

The energy distribution calculated is summarized in Table 5. For both Miscancell lignin runs, the energy recovery ranged from approximately 60 %–75 % of the initial energy content of the feedstock. The ORC represented the largest energy carrier (around 40 % of the energy recovery), followed by char and gases. Run 2 showed an improved energy recovery, which is consistent with its more balanced mass and carbon results. The lower gas energy observed in run 1 is in agreement with a possible underestimation of the gas phase during that experiment.

3.4. Product characterization

3.4.1. Pyrolysis condensates

Properties of bio-oils/ORCs from Indulin AT and Miscancell lignin can be seen in Table 6. The Indulin AT bio-oil has a very low water content of only 6.7 wt%, whereas the Miscancell oil has a higher water content of 12.5 wt%. The higher water content of the Miscancell lignin ORC may be attributed to the higher moisture content in the feedstock, as well as the decomposition of sugar impurities, which yields more water in its decomposition compared to lignin [39]. In addition, the condensation temperature profiles could also have influenced the results. The temperature of the first condensation stage was aimed at 90 °C

Table 5
Energy balances of lignin fast pyrolysis experiments (MJ/kg of dry feedstock).

	ORC	Char	Gases	Energy Recovery (%)
Miscancell #1	9.5	2.9	2.1	60
Miscancell #2	10.3	4.4	3.9	75

Table 6
Properties of organic-rich condensates (ORC).

Property	Indulin AT	Miscancell
Water content (wt. %)	6.7	12.5
Density at 60 °C (g/ml)	1.1521	1.1073
C[a] (wt. %)	68.3	60.4
H (wt. %)	6.9	6.1
N (wt. %)	1.4	2.7
S (wt. %)	0.0	0.0
O (wt. %)	23.5	30.7
HHV ($MJ \bullet kg^{-1}$)	29.9	25.6

[a] Elemental analysis data given on dry basis.

for all experiments. This was verified for the two successful runs with the Miscancell lignin; however, due to the short duration of the Indulin AT experiments, the temperature profiles might have encountered more significant fluctuations. Moreover, the composition of pyrolysis vapors and vapor-liquid equilibrium interactions during condensation can impact the amount of water that is condensed [24]. The density of the two oils is quite comparable, with Indulin AT oil at 1.1521 g/ml and Miscancell oil at 1.1073 g/ml, showing no significant difference. The elemental composition of the oils falls within the ranges documented in literature for lignin bio-oils [44,45]. The carbon content of the oils (60.4–68.3 wt%) aligns with values reported for lignin oils [44,45], and is notably higher than the carbon content typically found in bio-oils from whole biomass, which generally remains below 55 wt% [46]. Similarly, the oxygen content (23.5–30.7 wt%) is within the expected range for lignin pyrolysis oils [44,45] and is lower than the 35–40 wt% commonly observed in biomass-derived oils [46]. Comparing the oils, Indulin AT oil shows a higher carbon and lower oxygen content than Miscancell oil, which correlates to the feedstock characteristics, with Indulin AT being a more purified and richer in lignin, while Miscancell lignin appears to contain sugar impurities. The nitrogen content follows a similar trend, with Miscancell oil containing more nitrogen (2.7 wt%) than Indulin AT (1.4 wt%), also in line with the feedstock composition. Surprisingly, the Indulin AT oil does not show the presence of sulfur, which likely ended

up in the gases during the pyrolysis process [47]. The HHV values for the organic-rich condensate (ORC) of the lignin oils are in good agreement with those reported in the literature [44,45,48]. The HHV of lignin-derived bio-oils, typically around 30 MJ/kg, is notably higher compared to oils obtained from lignocellulosic biomass (usually around 17 MJ/kg [46,48]). This difference arises because lignin typically has a higher carbon content and lower oxygen content than lignocellulosic biomass, contributing to a greater energy density, making lignin-derived oils promising intermediates for upgrading into fuels.

Table 7 displays the main functional groups of compounds identified and quantified through GC-MS/FID in the pyrolysis condensates. Results are reported as approximate weight percentages. A detailed list of all the components and amounts identified in the analysis is available in the supporting information. Regarding the composition of the ORCs, the Indulin AT oil predominantly consist of phenols (6.2 ± 0.4 wt %) and guaiacols (11.4 ± 3.0 wt %), with guaiacol, creosol, isoeugenol, and phenol being the most prevalent compounds. There is no presence of syringol, as in the micro-pyrolysis experiments, due to the softwood nature of the biomass, and no sugar compounds in the oil, confirming the purified nature of this lignin. In contrast, the Miscancell lignin ORC shows both the presence of syringol, due to the grass nature of the lignin feedstock (that contains S, G and H units) and of sugar compounds (mainly levoglucosan), also confirming the result of the micro-pyrolysis experiments. Additionally, the Miscancell lignin ORC also exhibits the presence of acids (8.2 ± 0.1 wt %) and furans (0.4 ± 0.0 wt %), which are related to the degradation of sugars [39]. The total content of phenolic monomers of the Indulin AT oil is around 18 wt % which is slightly higher than for the Miscancell oil, which is around 14 wt %, which again correlates to the more purified nature of the Indulin AT lignin.

These profiles closely match the results obtained from the micro-pyrolysis (Py-GC/MS) experiments, where the same dominant phenolic monomers were identified. The agreement between the two techniques confirms that key structural features of the lignins were retained during fast pyrolysis and reinforces the reliability of the pilot-scale experiments in capturing the representative product distribution.

It is worth noting that, besides the water content, only about 20–27 wt% of the composition of the ORC could be identified through the GC-MS/FID analysis. This is due to the limitation of volatility of high molecular weight compounds that are often too heavy to be detected by standard GC-MS equipment [49]. This high molecular weight fraction of the bio-oil, often referred to as “pyrolytic lignin”, is composed of oligomers derived from the decomposition of lignin, which explains its significant presence in lignin-derived oils [50,51].

For the AC, the main components identified were non-aromatic organic acids for Miscancell and non-aromatic ketones for the Indulin AT. Small amounts of phenols, guaiacols and nitrogenated compounds were also encountered. These components are typically lower molecular weight compounds with lower boiling point, which are likely to condensate on the second condenser and end up on the AC, which operates near room temperature. In addition, Karl Fischer titration results show that the AC is composed of mainly water, 91.8 ± 1.0 wt % for the AC of Indulin AT and 92.6 ± 1.0 wt % for the AC of Miscancell.

Table 7
Main groups of compounds identified by GC-MS in organic-rich condensate (ORC) and aqueous condensate (AC).

	Indulin AT (wt. %)		Miscancell (wt. %)	
Compound	ORC	AC	ORC	AC
Non-aromatic Compounds				
Acids	0	0.3 ± 0.0	8.2 ± 0.1	1.1 ± 0.1
Ketones	0.7 ± 0.0	1.2 ± 0.2	1.4 ± 0.1	0.7 ± 0.1
Heterocyclic Compounds				
Furans	0.1 ± 0.0	0	0.4 ± 0.0	0.1 ± 0.0
Aromatic Compounds				
Benzene	0.4 ± 0.0	0	0.6 ± 0.0	0
Lignin-derived Phenol	6.2 ± 0.4	0.5 ± 0.0	3.9 ± 0.1	0.2 ± 0.0
Guaiacols (Methoxy Phenols)	11.4 ± 3.0	0.2 ± 0.0	6.1 ± 0.5	0.2 ± 0.0
Syringols (Dimethoxy Phenols)	0	0	3.6 ± 0.5	0
Carbohydrates				
Sugars	0	0	2.1 ± 0.1	0
Other Organic Compounds				
N-compounds	1.1 ± 0.2	1.0 ± 0.0	0.2 ± 0.0	0.5 ± 0.1

3.4.2. Char

Pyrolysis chars were analyzed for their elemental composition and ash content, HHV values were calculated based on the elemental composition. Table 8 shows the values obtained for the two Miscancell batches. Analysis shows that the char is rich in ash, which was anticipated given the high ash content of the Miscanthus feedstock. This elevated ash content affects the carbon content, resulting in lower-than-expected levels and also contributes to a lower higher heating value (HHV) compared to both the bio-oil and the feedstock. The low oxygen content, below 10 wt%, is consistent with reported values for pyrochar from other biomasses pyrolyzed in the unit [52]. The nitrogen content observed in the char was lower than the one observed in the bio-oil.

In addition to potential energetic use as a solid fuel, biochar is increasingly regarded as a valuable product for carbon removal and material applications. Lignin-derived chars, in particular, can exhibit high aromaticity and structural stability, making them promising for carbon sequestration and advanced uses [6].

3.4.3. Pyrolysis gases

Table 9 presents the composition of the non-condensable gases produced during the Miscancell lignin fast pyrolysis, expressed in volume percent of the total dry gas, and excluding the nitrogen supplied to create the inert environment required for the pyrolysis. The main components identified in the pyrolysis gases were carbon monoxide (CO), carbon dioxide (CO_2) and methane (CH_4), typical results for biomass and lignin fast pyrolysis [52,53]. The higher deviations that can be seen for the run of Miscancell batch #1 could be somehow related to the underestimation of gases during this run. Overall, the produced pyrolysis gases presents the primary components of syngas, making it suitable for energy generation.

4. Conclusion

This study investigated the use of a twin-screw reactor for the fast pyrolysis of lignin at a pilot scale, comparing the performance and resulting bio-oils of two types of lignin: Indulin AT, a Kraft lignin, and Miscancell, a *Miscanthus*-derived alkali lignin. The effectiveness of this type of reactor was evaluated based on its ability to process the lignins and the properties and composition of the bio-oils produced.

Initial tests with the original reactor setup, where the feedstock entered at the cold inlet of the screw and the heat carrier was added later, revealed significant challenges with Indulin AT, leading to severe agglomeration inside the reactor. Modifications to the reactor inlet, which reversed the order of biomass and heat carried, successfully minimized blockage inside the reactor. This confirmed the hypothesis that the mechanical forces associated with the twin-screw reactor could break up agglomerates formed during lignin pyrolysis. However, a new issue arose with agglomerates building up at the biomass feeding drop

Table 8
Elemental analysis and ash content of Miscancell lignin chars (dry basis).

Char	C (wt. %)	H (wt. %)	O (wt. %)	N (wt. %)	Ash (wt. %)	HHV (MJ/kg)
Miscancell #1	56.3	2.4	9.5	1.5	30.4	20.6
Miscancell #2	58.9	2.3	7.1	1.5	30.3	21.7

Table 9
Lignin fast pyrolysis gas composition (N_2 free, dry basis).

	H_2 (vol %)	CO (vol %)	CO_2 (vol %)	CH_4 (vol %)	C_2-C_5+ (vol %)
Miscancell #1	7.3 ± 1.3	27.7 ± 2.3	45.2 ± 3.7	15.7 ± 1.6	5.7 ± 0.6
Miscancell #2	6.6 ± 0.1	29.4 ± 1.2	45.7 ± 2.6	15.2 ± 0.5	6.1 ± 0.3

pipe during the pyrolysis of Indulin AT. In contrast, processing of the Miscancell lignin in the modified reactor setup proceeded smoothly without any plugging or significant material deposition, highlighting its potential as a suitable feedstock for fast pyrolysis. The pilot runs with Miscancell lignin yielded little organic liquids; however, the observed yields were in line with results from feedstock with a similar high ash content. The differences in processing behavior between the two lignins can be attributed to their distinct chemical nature and physicochemical properties. Analysis of the oils showed that, Indulin AT produced a phenolic-rich oil, composed of mainly phenols and guaiacols, while the Miscancell lignin generated a broader range of components, including syringols, sugars, and furans, suggesting the presence of sugar impurities. Additionally, the consistency between the oil analysis and micro-pyrolysis experiments provides validation of the pilot-scale runs and its operational reliability.

These findings suggest that the twin-screw reactor design used in the study is effective for breaking up agglomerates during lignin pyrolysis, proving its suitability for this process. Still, further investigation is necessary to optimize feeding conditions for Indulin AT lignin and other lignins with pronounced melting behavior. Ultimately, Miscancell lignin and other lignins that do not exhibit severe melting behavior stand out as promising candidates for conversion via fast pyrolysis, due to their smooth processing and lack of operational issues.

CRediT authorship contribution statement

Ana Cristina Corrêa de Araujo: Writing – original draft, Investigation, Data curation. **Axel Funke:** Writing – review & editing, Supervision, Conceptualization. **Antigoni Margellou:** Writing – review & editing, Methodology, Investigation. **Konstantinos Triantafyllidis:** Writing – review & editing, Supervision, Project administration, Conceptualization. **Nicolaus Dahmen:** Supervision, Funding acquisition.

Acknowledgements

This study was supported by the European Union's Horizon 2020 research and innovation programme under Grant Agreement No. 101007130. The authors thank Norbert Sickinger for designing the changes in the pilot unit and Daniel Richter for performing these changes and conducting the fast pyrolysis experiments.

Appendix A. Supplementary data

Supplementary data to this article can be found online at https://doi.org/10.1016/j.biombioe.2025.108041.

Data availability

Data will be made available on request.

References

[1] C.C. Zandonadi Nunes, H.B. De Paula, I.F. Demuner, M.O. De Paula, L.G. Pedroti, A.M.M.L. Carvalho, Kraft lignin biorefinery: from pulping side streams to concrete plasticizers, Eur. J. Wood Prod. 82 (2024) 849–860, https://doi.org/10.1007/s00107-024-02044-8.
[2] S. Suresh, V. Viswanathan, M. Angamuthu, G.P. Dhakshinamoorthy, K.P. Gopinath, A. Bhatnagar, Lignin waste processing into solid, liquid, and gaseous fuels: a comprehensive review, Biomass Conv. Bioref. 13 (2023) 4515–4553, https://doi.org/10.1007/s13399-021-01497-8.
[3] F.F. Menezes, V.M. Nascimento, G.R. Gomes, GeorgeJ.M. Rocha, M. Strauss, T. L. Junqueira, C. Driemeier, Depolymerization of enzymatic hydrolysis lignin: review of technologies and opportunities for research, Fuel (Guildf.) 342 (2023) 127796, https://doi.org/10.1016/j.fuel.2023.127796.
[4] A.G. Margellou, P.A. Lazaridis, I.D. Charisteidis, C.K. Nitsos, C.P. Pappa, A. P. Fotopoulos, S. Van Den Bosch, B.F. Sels, K.S. Triantafyllidis, Catalytic fast pyrolysis of beech wood lignin isolated by different biomass (pre)treatment processes: organosolv, hydrothermal and enzymatic hydrolysis, Appl. Catal. Gen. 623 (2021) 118298, https://doi.org/10.1016/j.apcata.2021.118298.
[5] P. Soldatos, A. Margellou, C. Pappa, S. Torofias, L. Matsakas, U. Rova, P. Christakopoulos, K. Triantafyllidis, Conversion of beechwood organosolv lignin via fast pyrolysis and in situ catalytic upgrading towards aromatic and phenolic-rich bio-oil, Sustainable Chemistry for the Environment 6 (2024) 100107, https://doi.org/10.1016/j.scenv.2024.100107.
[6] G.R. Gomes, E.G. De Jesus, J.C.C. Jacintho, D.L.G. García, B.R.A. Alencar, F. P. Gabetto, J.J. Gomes, J.L.N. Carvalho, M. Strauss, C. Driemeier, Peculiarities of bio-oil and biochar obtained from the lignin-rich residue of the enzymatic hydrolysis of sugarcane bagasse, Renew. Energy 241 (2025) 122282, https://doi.org/10.1016/j.renene.2024.122282.
[7] B. Shrestha, Y. Le Brech, T. Ghislain, S. Leclerc, V. Carré, F. Aubriet, S. Hoppe, P. Marchal, S. Pontvianne, N. Brosse, A. Dufour, A multitechnique characterization of lignin softening and pyrolysis, ACS Sustainable Chem. Eng. 5 (2017) 6940–6949, https://doi.org/10.1021/acssuschemeng.7b01130.
[8] D.J. Nowakowski, A.V. Bridgwater, D.C. Elliott, D. Meier, P. de Wild, Lignin fast pyrolysis: results from an international collaboration, J. Anal. Appl. Pyrolysis 88 (2010) 53–72, https://doi.org/10.1016/j.jaap.2010.02.009.
[9] S. Zhou, R.C. Brown, X. Bai, The use of calcium hydroxide pretreatment to overcome agglomeration of technical lignin during fast pyrolysis, Green Chem. 17 (2015) 4748–4759, https://doi.org/10.1039/C5GC01611H.
[10] S. Ghysels, B. Dubuisson, M. Pala, L. Rohrbach, J. Van Den Bulcke, H.J. Heeres, F. Ronsse, Improving fast pyrolysis of lignin using three additives with different modes of action, Green Chem. 22 (2020) 6471–6488, https://doi.org/10.1039/D0GC02417A.
[11] P.J. de Wild, W.J.J. Huijgen, H.J. Heeres, Pyrolysis of wheat straw-derived organosolv lignin, J. Anal. Appl. Pyrolysis 93 (2012) 95–103, https://doi.org/10.1016/j.jaap.2011.10.002.
[12] A. Tumbalam Gooty, D. Li, F. Berruti, C. Briens, Kraft-lignin pyrolysis and fractional condensation of its bio-oil vapors, J. Anal. Appl. Pyrolysis 106 (2014) 33–40, https://doi.org/10.1016/j.jaap.2013.12.006.
[13] D. Li, C. Briens, F. Berruti, Improved lignin pyrolysis for phenolics production in a bubbling bed reactor – effect of bed materials, Bioresour. Technol. 189 (2015) 7–14, https://doi.org/10.1016/j.biortech.2015.04.004.
[14] A. Singh-Morgan, A. Puente-Urbina, J.A. van Bokhoven, Technology overview of fast pyrolysis of lignin: current state and potential for scale-up, ChemSusChem 15 (2022) e202200343, https://doi.org/10.1002/cssc.202200343.
[15] E. Pienihäkkinen, C. Lindfors, T. Ohra-aho, J. Lehtonen, T. Granström, M. Yamamoto, A. Oasmaa, Fast pyrolysis of hydrolysis lignin in fluidized bed reactors, Energy Fuel. 35 (2021) 14758–14769, https://doi.org/10.1021/acs.energyfuels.1c01719.
[16] H. Shafaghat, P.S. Rezaei, D. Ro, J. Jae, B.-S. Kim, S.-C. Jung, B.H. Sung, Y.-K. Park, In-situ catalytic pyrolysis of lignin in a bench-scale fixed bed pyrolyzer, J. Ind. Eng. Chem. 54 (2017) 447–453, https://doi.org/10.1016/j.jiec.2017.06.026.
[17] I. Charisteidis, P. Lazaridis, A. Fotopoulos, E. Pachatouridou, L. Matsakas, U. Rova, P. Christakopoulos, K. Triantafyllidis, Catalytic fast pyrolysis of lignin isolated by hybrid organosolv—steam explosion pretreatment of hardwood and softwood biomass for the production of phenolics and aromatics, Catalysts 9 (2019) 935, https://doi.org/10.3390/catal9110935.
[18] T.N. Trinh, P.A. Jensen, Z. Sárossy, K. Dam-Johansen, N.O. Knudsen, H. R. Sørensen, H. Egsgaard, Fast pyrolysis of lignin using a pyrolysis centrifuge reactor, Energy Fuel. 27 (2013) 3802–3810, https://doi.org/10.1021/ef400527k.
[19] S. Mukkamala, M.C. Wheeler, A.R.P. Van Heiningen, W.J. DeSisto, Formate-assisted fast pyrolysis of lignin, Energy Fuel. 26 (2012) 1380–1384, https://doi.org/10.1021/ef201756a.
[20] F. Campuzano, R.C. Brown, J.D. Martínez, Auger reactors for pyrolysis of biomass and wastes, Renew. Sustain. Energy Rev. 102 (2019) 372–409, https://doi.org/10.1016/j.rser.2018.12.014.
[21] A. Funke, M. Tomasi Morgano, N. Dahmen, H. Leibold, Experimental comparison of two bench scale units for fast and intermediate pyrolysis, J. Anal. Appl. Pyrolysis 124 (2017) 504–514, https://doi.org/10.1016/j.jaap.2016.12.033.
[22] S.-S. Liaw, Z. Wang, P. Ndegwa, C. Frear, S. Ha, C.-Z. Li, M. Garcia-Perez, Effect of pyrolysis temperature on the yield and properties of bio-oils obtained from the auger pyrolysis of Douglas Fir wood, J. Anal. Appl. Pyrolysis 93 (2012) 52–62, https://doi.org/10.1016/j.jaap.2011.09.011.
[23] A. Niebel, A. Funke, C. Pfitzer, N. Dahmen, N. Weih, D. Richter, B. Zimmerlin, Fast pyrolysis of wheat straw—improvements of operational stability in 10 Years of bioliq pilot plant operation, Energy Fuel. 35 (2021) 11333–11345, https://doi.org/10.1021/acs.energyfuels.1c00851.
[24] N. Weih, A. Niebel, C. Pfitzer, A. Funke, G.K. Parku, N. Dahmen, Operational experience with miscanthus feedstock at the bioliq® fast pyrolysis plant, J. Anal. Appl. Pyrolysis 177 (2024) 106338, https://doi.org/10.1016/j.jaap.2023.106338.

[25] E. Henrich, N. Dahmen, F. Weirich, R. Reimert, C. Kornmayer, Fast pyrolysis of lignocellulosics in a twin screw mixer reactor, Fuel Process. Technol. 143 (2016) 151–161, https://doi.org/10.1016/j.fuproc.2015.11.003.
[26] A. Funke, D. Richter, A. Niebel, N. Dahmen, J. Sauer, Fast pyrolysis of biomass residues in a twin-screw mixing reactor, JoVE J. (2016) 54395, https://doi.org/10.3791/54395.
[27] A. Demirbaş, Calculation of higher heating values of biomass fuels, Fuel (Guildf.) 76 (1997) 431–434, https://doi.org/10.1016/S0016-2361(97)85520-2.
[28] M. Windt, D. Meier, J.H. Marsman, H.J. Heeres, S. De Koning, Micro-pyrolysis of technical lignins in a new modular rig and product analysis by GC–MS/FID and GC×GC–TOFMS/FID, J. Anal. Appl. Pyrolysis 85 (2009) 38–46, https://doi.org/10.1016/j.jaap.2008.11.011.
[29] B. Dubis, K. Bułkowska, M. Lewandowska, W. Szempliński, K.J. Jankowski, J. Idźkowski, N. Kordala, K. Szymańska, Effect of different nitrogen fertilizer treatments on the conversion of Miscanthus×giganteus to ethanol, Bioresour. Technol. 243 (2017) 731–737, https://doi.org/10.1016/j.biortech.2017.07.005.
[30] N. Brosse, A. Dufour, X. Meng, Q. Sun, A. Ragauskas, *Miscanthus* : a fast-growing crop for biofuels and chemicals production, Biofuel Bioprod. Biorefining 6 (2012) 580–598, https://doi.org/10.1002/bbb.1353.
[31] K.P. Woli, M.B. David, J. Tsai, T.B. Voigt, R.G. Darmody, C.A. Mitchell, Evaluating silicon concentrations in biofuel feedstock crops Miscanthus and switchgrass, Biomass Bioenergy 35 (2011) 2807–2813, https://doi.org/10.1016/j.biombioe.2011.03.007.
[32] T. Han, N. Sophonrat, A. Tagami, O. Sevastyanova, P. Mellin, W. Yang, Characterization of lignin at pre-pyrolysis temperature to investigate its melting problem, Fuel (Guildf.) 235 (2019) 1061–1069, https://doi.org/10.1016/j.fuel.2018.08.120.
[33] M.E. Moustaqim, A.E. Kaihal, M.E. Marouani, S. Men-La-Yakhaf, M. Taibi, S. Sebbahi, S.E. Hajjaji, F. Kifani-Sahban, Thermal and thermomechanical analyses of lignin, Sustain. Chem. Pharm. 9 (2018) 63–68, https://doi.org/10.1016/j.scp.2018.06.002.
[34] D.R. Naron, F.-X. Collard, L. Tyhoda, J.F. Görgens, Production of phenols from pyrolysis of sugarcane bagasse lignin: catalyst screening using thermogravimetric analysis – thermal desorption – gas chromatography – mass spectroscopy, J. Anal. Appl. Pyrolysis 138 (2019) 120–131, https://doi.org/10.1016/j.jaap.2018.12.015.
[35] E. Jakab, Analytical techniques as a tool to understand the reaction mechanism, in: Recent Advances in Thermo-Chemical Conversion of Biomass, Elsevier, 2015, pp. 75–108, https://doi.org/10.1016/B978-0-444-63289-0.00003-X.
[36] J. Domínguez-Robles, E. Espinosa, D. Savy, A. Rosal, A. Rodriguez, Biorefinery process combining Specel® process and selective lignin precipitation using mineral acids, Bioresources 11 (2016) 7061–7077, https://doi.org/10.15376/biores.11.3.7061-7077.
[37] S. Zhou, Y. Xue, A. Sharma, X. Bai, Lignin valorization through thermochemical conversion: comparison of hardwood, softwood and herbaceous lignin, ACS Sustainable Chem. Eng. 4 (2016) 6608–6617, https://doi.org/10.1021/acssuschemeng.6b01488.
[38] P.A. Lazaridis, A.P. Fotopoulos, S.A. Karakoulia, K.S. Triantafyllidis, Catalytic fast pyrolysis of Kraft lignin with conventional, mesoporous and nanosized ZSM-5 zeolite for the production of alkyl-phenols and aromatics, Front. Chem. 6 (2018) 295, https://doi.org/10.3389/fchem.2018.00295.
[39] A. Aho, N. Kumar, K. Eränen, B. Holmbom, M. Hupa, T. Salmi, D.Yu Murzin, Pyrolysis of softwood carbohydrates in a fluidized bed reactor, IJMS 9 (2008) 1665–1675, https://doi.org/10.3390/ijms9091665.
[40] M. Bergs, G. Völkering, T. Kraska, R. Pude, X.T. Do, P. Kusch, Y. Monakhova, C. Konow, M. Schulze, Miscanthus x giganteus stem versus leaf-derived lignins differing in monolignol ratio and linkage, IJMS 20 (2019) 1200, https://doi.org/10.3390/ijms20051200.
[41] M. Bergs, X.T. Do, J. Rumpf, P. Kusch, Y. Monakhova, C. Konow, G. Völkering, R. Pude, M. Schulze, Comparing chemical composition and lignin structure of *Miscanthus x giganteus* and *Miscanthus nagara* harvested in autumn and spring and separated into stems and leaves, RSC Adv. 10 (2020) 10740–10751, https://doi.org/10.1039/C9RA10576J.
[42] P.S. Marathe, R.J.M. Westerhof, S.R.A. Kersten, Fast pyrolysis of lignins with different molecular weight: experiments and modelling, Appl. Energy 236 (2019) 1125–1137, https://doi.org/10.1016/j.apenergy.2018.12.058.
[43] F.G. Fonseca, A. Anca-Couce, A. Funke, N. Dahmen, Challenges in kinetic parameter determination for wheat straw pyrolysis, Energies 15 (2022) 7240, https://doi.org/10.3390/en15197240.
[44] A. Moutsoglou, B. Lawburgh, J. Lawburgh, Fractional condensation and aging of pyrolysis oil from softwood and organosolv lignin, J. Anal. Appl. Pyrolysis 135 (2018) 350–360, https://doi.org/10.1016/j.jaap.2018.08.016.
[45] T.N. Trinh, P.A. Jensen, K. Dam-Johansen, N.O. Knudsen, H.R. Sørensen, S. Hvilsted, Comparison of lignin, macroalgae, wood, and straw fast pyrolysis, Energy Fuel. 27 (2013) 1399–1409, https://doi.org/10.1021/ef301927y.
[46] A.V. Bridgwater, Review of fast pyrolysis of biomass and product upgrading, Biomass Bioenergy 38 (2012) 68–94, https://doi.org/10.1016/j.biombioe.2011.01.048.
[47] M. Borella, A.A. Casazza, G. Garbarino, P. Riani, G. Busca, A study of the pyrolysis products of Kraft lignin, Energies 15 (2022) 991, https://doi.org/10.3390/en15030991.
[48] J. Gracia-Vitoria, S.C. Gándara, E. Feghali, P. Ortiz, W. Eevers, K.S. Triantafyllidis, K. Vanbroekhoven, The chemical and physical properties of lignin bio-oils, facts and needs, Curr. Opin. Green Sustainable Chem. 40 (2023) 100781, https://doi.org/10.1016/j.cogsc.2023.100781.
[49] W. Mu, H. Ben, A. Ragauskas, Y. Deng, Lignin pyrolysis components and upgrading—technology review, Bioenerg. Res. 6 (2013) 1183–1204, https://doi.org/10.1007/s12155-013-9314-7.
[50] B. Scholze, D. Meier, Characterization of the water-insoluble fraction from pyrolysis oil (pyrolytic lignin). Part I. PY–GC/MS, FTIR, and functional groups, J. Anal. Appl. Pyrolysis 60 (2001) 41–54, https://doi.org/10.1016/S0165-2370(00)00110-8.
[51] F.G. Fonseca, A. Funke, Modeling of liquid–vapor phase equilibria of pyrolysis bio-oils: a review, Ind. Eng. Chem. Res. 63 (2024) 13401–13420, https://doi.org/10.1021/acs.iecr.4c00775.
[52] J.O. Ajikashile, M.-J. Alhnidi, G.K. Parku, A. Funke, A. Kruse, A study on the fast pyrolysis of millet and sorghum straws sourced from arid and semi-arid regions of Nigeria in a twin-screw mixing reactor, Mater. Sci. Energy Technol. 6 (2023) 388–398, https://doi.org/10.1016/j.mset.2023.03.007.
[53] S.H. Beis, S. Mukkamala, N. Hill, J. Joseph, C. Baker, B. Jensen, E.A. Stemmler, C. Wheeler, B.G. Frederick, A. Van Heiningen, A.G. Berg, W.J. DeSisto, Fast pyrolysis of lignins, Bio 5 (2010) 1408–1424, https://doi.org/10.15376/biores.5.3.1408-1424.